Soft Collective Fluctuations Governing Hydrophobic Association

Aljaž Godec,[1,2,*] Jeremy C. Smith,[3,4] and Franci Merzel[1,†]

[1]*National Institute of Chemistry, Hajdrihova 19, 1000 Ljubljana, Slovenia*
[2]*Institute for Physics and Astronomy, University of Potsdam, 14476 Potsdam-Golm, Germany*
[3]*UT/ORNL Center for Molecular Biophysics, Post Office Box 2008, Oak Ridge, Tennessee 37831-6309, USA*
[4]*Department of Biochemistry and Cellular and Molecular Biology, University of Tennessee, M407 Walters Life Sciences, 1414 Cumberland Avenue, Knoxville, Tennessee 37996, USA*

(Received 21 February 2013; revised manuscript received 2 August 2013; published 18 September 2013)

The interaction between two associating hydrophobic particles has traditionally been explained in terms of the release of entropically frustrated hydration shell water molecules. However, this picture cannot account for the kinetics of hydrophobic association and is therefore not capable of providing a microscopic description of the hydrophobic interaction (HI). Here, Monte Carlo simulations of a pair of molecular-scale apolar solutes in aqueous solution reveal the critical role of collective fluctuations in the hydrogen bond (HB) network for the microscopic picture of the HI. The main contribution to the HI is the relaxation of solute-water translational correlations. The existence of a heat capacity maximum at the desolvation barrier is shown to arise from softening of non-HB water fluctuations and the relaxation of many-body correlations in the labile HB network. The microscopic event governing the kinetics of hydrophobic association has turned out to be a relatively large critical collective fluctuation in hydration water displacing a substantial fraction of HB clusters from the inner to the outer region of the first hydration shell.

DOI: 10.1103/PhysRevLett.111.127801 PACS numbers: 61.20.−p, 05.20.Jj, 68.35.Rh, 82.30.Rs

Hydration of apolar molecules [1] is associated with a loss in entropy, which is commonly attributed to the reduction of the configuration space available to single-water molecules if they are to maintain hydrogen bonding (HB) [2,3]. The entropy-driven association of apolar molecules is referred to as the hydrophobic interaction (HI) and has been confirmed in a vast variety of studies (see, for example, Refs. [4,5]). The source of attraction is assumed to be the release of entropically constrained water molecules into the bulk such that the accompanying entropic change is favorable [2,6].

The free energy of the HI as a function of interparticle separation has been investigated on numerous occasions, both computationally [2,6,7] and experimentally [8]. Simulations indicate that the HI has a global minimum at the contact distance and a second, shallow minimum at a distance at which interacting particles are separated by a water molecule [4,6,7]. Separating the two minima is a desolvation barrier (DB), as shown in Fig. 1(a), and at this point, the excess heat capacity has been found to be a maximum as a function of the interparticle distance [4,6,7]. An understanding of the microscopic origin of this "activation" barrier would provide the basis for an explanation of the kinetics driven by the HI.

Numerous detailed studies have been performed of the macroscopic thermodynamic features of the HI [6,7,9], which can also be characterized theoretically using, for example, scaled particle theory [10], information theory [5], or the Lum-Chandler-Weeks theory [11]. However, the microscopic physical principles involved are incompletely understood. There is clear experimental and theoretical evidence that the molecular reorientation underlying the exchange of hydrogen bonds is not continuous diffusion but occurs as sudden large-amplitude jumps [12,13]. This in turn means that in between HB exchange events, a water molecule, which is essentially part of a labile, dynamic HB network, spends most of its time hydrogen bonded to two or more of its nearest neighbors while undergoing librational-type fluctuations. Hence, the features of water reorganization leading to the HI may be best describable in terms of fluctuations of the (labile) HB network involving concerted many-body effects [14].

To determine the generic microscopic picture of the HI, we investigate the behavior of structural order and

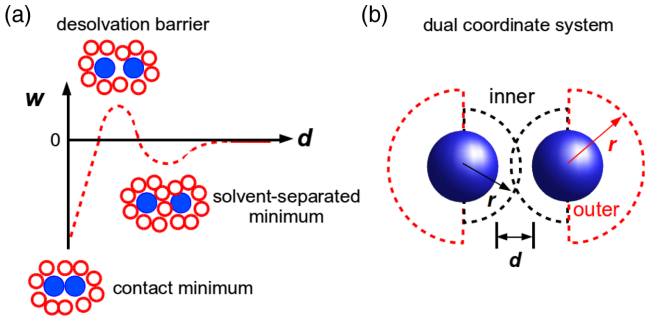

FIG. 1 (color online). (a) Schematic free energy $w(d)$ as a function of distance between two apolar particles in aqueous solutions. (b) A schematic of the dual coordinate system introducing the inner and outer regions of hydration space surrounding two hydrophobic solutes (blue spheres).

fluctuations when two molecular-scale model apolar particles of two types are brought into contact. We perform constant pressure Monte Carlo simulation with the five-site point charge water model TIP5P [15] and pairs of (i) hard spheres (HS) and (ii) solvent attracting hard spheres (SAHS) in an orthogonal simulation box with periodic boundary conditions. We consider 11 systems per solute type with the two solutes freely moving at fixed interparticle distances ranging from close contact to an intersurface distance of 15 Å at $p = 1$ bar and $T = 300$ K. The hard sphere diameter for the HS system is taken to be 2.8 Å (∼ the diameter of a water molecule) and 3.6 Å for the SAHS system (∼ the diameter of a methane molecule) in which an attractive tail $-\varepsilon/r^6$ is appended to the hard repulsion. ε is set to $4.2k_BT$ Å^6 to roughly mimic the methane-water potential. The systems consist of 3739–4700 water molecules depending on the interparticle separation. After an equilibration period, as many trial moves were performed as were needed to assure that on average each molecule was moved 4×10^5 times at the acceptance rate of 30%. For the analysis, we introduce a dual coordinate system which divides the hydration space into two pairs of semishells [see the schematic in Fig. 1(b)], each comprising a closed effective shell on realignment. As we will show, differences in behavior of water molecules in the inner and outer regions of the first hydration shell are critical to the HI. In what follows, we present results for the HS system, mentioning the effects of solute-water attractions where appropriate.

We first address the local environment of water molecules inside the inner and outer regions of the first hydration shell. Instead of the usual distance cutoff for close contact and HB neighbors of 3.5 Å [6,12], we use 3 Å, as it has been shown that there is no preferential mutual orientation between two water molecules if they are more than 3 Å apart (see the Supplemental Material [16] and Ref. [17]). Our choice gives for bulk water an average of just over three close contacts of which just over two are HB. The structure of the hydration water, as revealed from nearest neighbor distributions per water molecule in Fig. S5 in the Supplemental Material [16], does not vary notably with interparticle distance, except that the distributions are somewhat wider when the particles are closer, indicating enhanced fluctuations in the HB network, i.e., increased diversity of local environments. The structural invariance with respect to interparticle distance is robust, as we find no significant differences between the HS and SAHS systems. Both the average number of close contacts and HB neighbors (denoted by circles) are almost independent of the interparticle separation. Also, the structure of the inner region does not differ from the outer one. Figure 2(a) shows that the occupancy of the first shell is sensitive to the interparticle separation. The variations in $\langle N \rangle(d)$ may be assumed to be a consequence of the local water packing and the commensurability of the

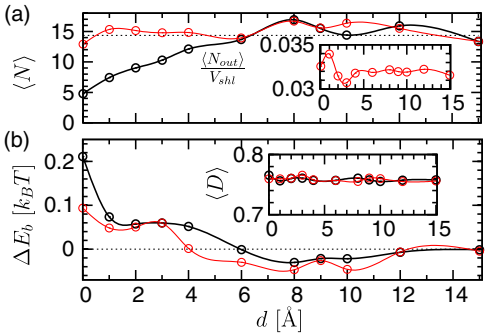

FIG. 2 (color online). (a) The average number of water molecules in the inner (black) and outer dark gray (red) parts of the first hydration shell as a function of d. The dashed line denotes the results for $d = \infty$. Inset: The approximate packing density in the outer region of the first hydration shell. (b) The difference in the binding energy of a water molecule in the first hydration shell with respect to $d = \infty$, ΔE_b, where $E_b \equiv (1/2)\langle \sum_{i=1}^{N} u^{0i} \rangle$, with u being the sum of the Coulomb and van der Waals potential energies and the bar denoting an average over all molecules 0 in the first hydration shell. Inset: Average dipolar order parameter $\langle D \rangle$ of water molecules in the first hydration shells.

interparticle separation with the HB network topology. For $d < 6$ Å, the profiles for the inner and outer regions bifurcate as a consequence of the exclusion of inner shell molecules. In the case of a pair of HS, the packing density of the outer region ($\langle N_{\text{out}} \rangle / V_{\text{shl}}$) is highest at $d = 1$ Å and lowest at $d \sim 3$ Å. For the SAHS, we find exactly the same features [see Fig. S6(a) in the Supplemental Material [16]], albeit shifted slightly due to a larger particle size. For $d \geq 6$ Å, the difference in binding energy [Fig. 2(b) and Fig. S6 (b) in the Supplemental Material [16]] with respect to $d = \infty$, $\Delta E_b = E_b(d) - E_b(\infty)$, is negative, indicating stronger binding and thus on average a more favorable local environment. For $d < 4$ Å, the binding is less favorable and gets even weaker upon contact formation. Meanwhile, the average dipolar orientational order parameter $\langle D \rangle$ (see the Supplemental Material [16] and Ref. [17]) is apparently insensitive to variations of the intersurface separation.

We expect that due to the water exclusion process, the largest contribution to the HI comes from translational correlations between the solute and water molecules. Hence, we examine center-of-mass pair correlations, which we quantify in terms of the translational pair correlation entropy S_{tr}^c which expresses the level of positional stabilization of the solvent with respect to the solute. Adopting the positive sign for the correlation entropy, we define it as

$$S_{\text{tr},i}^c = \rho_B k_B \int g_{\text{sw}}^i(r) \ln g_{\text{sw}}^i(r) \frac{dV^i(r)}{dr} dr, \qquad (1)$$

where $g_{\text{sw}}^i(r)$ is the solute-water proximity correlation function for the region i (inner, outer) defined in terms of

the average number density of molecules at a distance r from the nearest solute center at $\boldsymbol{r}_s$, ρ_B is the number density of bulk water [i.e., $\rho_B = \rho(r = \infty)$], and $V^i(r)$ is the solvent available volume (see the Supplemental Material [16] for details). The results for $S^c_{\rm tr}$, represented as differences with respect to $d = \infty$, for the inner (black lines) and outer [dark gray (red) lines] region as well as the sum [medium gray (blue) lines] for a pair of HS, are shown in Fig. 3(a). As expected, the total $\Delta S^c_{\rm tr}$ exhibits the two minima separated by a DB at ~1 Å. We find that the DB is in fact due to very strong correlations in the outer region. Thus, the removal of molecules from the inner region causes more compact packing along with stronger correlations in the outer region [see the inset of Figs. 2(b) and 3(a)]. Meanwhile, the favorable contact formation is exclusively due to the release of inner molecules. Equivalent results are obtained for the SAHS pair (see Fig. S7 in the Supplemental Material [16]), with the positions of the minima and maxima shifted correspondingly, due to the larger particle size. The SAHS also has a higher DB and a lower contact minimum, a straightforward consequence of the solute-water attraction.

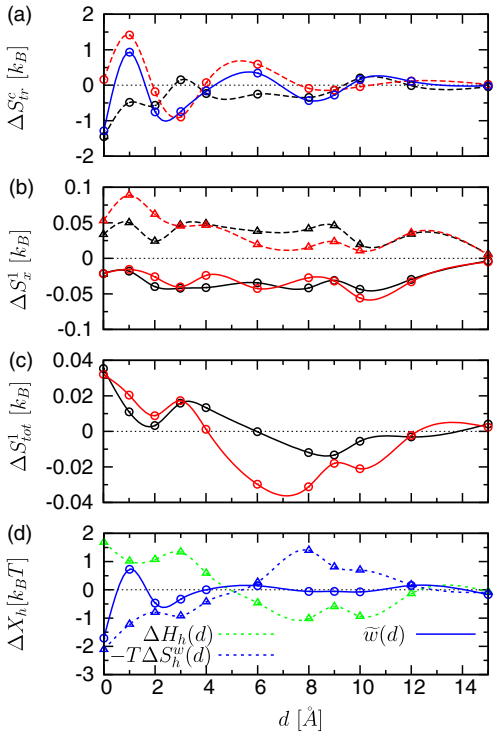

FIG. 3 (color online). (a) Solute-water pair translational correlation entropy difference: inner shell (black lines), outer shell [dark gray (red) lines], and the sum [medium gray (blue) lines]. (b) Non-HB (dashed lines) and HB (solid lines) fluctuation entropy difference. (c) Fluctuation entropy difference of the interaction with nearest neighbors. (d) The energetic contribution to the HI interaction free energy [light gray (green) dashed line], the contribution of fluctuation entropy of the interaction with nearest neighbors [medium gray (blue) dashed line], and the approximate HI potential $\tilde{w}(d)$ [medium gray (blue) solid line]. All quantities are expressed as a function of d relative to their values at $d = \infty$.

In order to further examine the behavior of water around apolar solutes, we focus on the interaction potential energies of pairs of water molecules that are either hydrogen bonded or not, as demonstrated in Ref. [14]. Using the random variable transformation theorem [18], we can always map the full configurational probability density, expressed in terms of the position and orientation of a given single molecule $\boldsymbol{\omega}$ onto a joint probability density for observing a given interaction potential energy U of pairs of molecules: $P(\boldsymbol{\omega}^N) = \exp[-\beta U(\boldsymbol{\omega}^N)]/Z$, where $\beta = 1/k_BT$ and Z is the configurational integral. For example, the joint probability density of two nearby pairs of kind x and y (x, $y = \{\text{HB, non-HB}\}$) having interaction energies u_x and u_y, given that a tagged molecule is located in the region z (z = inner, outer), can be exactly formulated as $\tilde{p}(u_x, u_y)$ (see the Supplemental Material [16]). In the simplest case, such an expression defines the probability density for observing a given pair interaction potential energy of kind x, $\tilde{p}(u_x)$, and can be used to quantify the extent of fluctuations of (non-)HB pairs with the Gibbs-Shannon entropy $S_x = -k_B \int \tilde{p}(u_x) \ln \tilde{p}(u_x) du_x$. The extent of librational fluctuations can be successfully used as a measure of HB strengthening [19]. Furthermore, we can define various joint probability densities $\tilde{p}(u_x, u_y)$ involving three or four molecules. $\tilde{p}(u_x, u_y)$ enables the evaluation of many-body correlations using the Kullback-Leibler correlation entropy [$S^c_{x,y} = S(x) + S(y) - S(x, y)$],

$$S^c_{x,y} = k_B \iint \tilde{p}(u_x, u_y) \ln \frac{\tilde{p}(u_x, u_y)}{\tilde{p}(u_x)\tilde{p}(u_y)} du_x du_y. \qquad (2)$$

The extension to more than four molecules is straightforward. With the exception of some approximate calculations of triplet correlations [20], many-body correlations have been hitherto systematically neglected [21].

For the HS system, S_x in Fig. 3(b) shows that there exists a lower HB fluctuation entropy for $d \leq 14$ Å, indicating HB strengthening in hydration water on a solute approach, in agreement with previous observations [6]. In the same range as that over which the HI becomes active, we also find enhanced fluctuations of non-HB interaction energies, suggesting a softening of non-HB pair fluctuations, this being most marked at the DB, at which point it is larger in the outer region.

Meanwhile, the fluctuation of the total interaction energy with nearest neighbors $S^{1,i}_{\rm tot}$ [Fig. 3(c)], which corresponds to coupled translational and orientational correlations of water molecule 1 with its closest neighbors and is a measure of the configuration space available to single molecules, is decreased for $d >$ ~4 Å. Note that $S^{1,i}_{\rm tot}$ ipso facto includes contributions of orientational correlations with respect to the solutes.

A comparison of the total contribution of the energetic component (i.e., the binding energy)

$$\Delta H_h(d) = \sum_{i=\text{in, out}} \{\langle N^i(d)\rangle[E_b^i(d) - E_{b,\text{bulk}}] - \langle N^i(\infty)\rangle \times [E_b^i(\infty) - E_{b,\text{bulk}}]\}$$

and the contribution of the single-water fluctuation entropy

$$-T\Delta S_h^w(d) = -T \sum_{i=\text{in, out}} \{\langle N^i(d)\rangle[S_{\text{tot}}^{1,i}(d) - S_{\text{tot, bulk}}^1] - \langle N^i(\infty)\rangle[S_{\text{tot}}^{1,i}(\infty) - S_{\text{tot, bulk}}^1]\},$$

shown in Fig. 3(d) [light gray and medium gray (green and blue) dashed lines], reveals that these two contributions almost completely balance each other out. By adding the contribution of the translational correlation entropy, we obtain an estimate for the HI potential $\tilde{w}(d) \approx \Delta H_h(d) - T\Delta S_h^w(d) + T\Delta S_{\text{tr}}^c(d)$, shown in Fig. 3(d) [medium gray (blue) solid line]. The shape of $\tilde{w}(d)$ is in agreement with those found in the literature [4,6,7]. However, the result is obtained in an entirely different manner, allowing decomposition of the HI potential into physically meaningful contributions. Although two particles feel no hydrophobic attraction for $d > 4$ Å, the surrounding hydration shells are nevertheless already perturbed at $d \sim 12$ Å [see Figs. 2(c), 3(a), and 3(b)]. The SAHS system exhibits the same generic features (see Fig. S7 in the Supplemental Material [16]). Here, ΔH_h is somewhat larger in magnitude than $-T\Delta S_h^w$ for $d < 4$ Å and compensates the larger magnitude of S_{tr}^c. These differences just about summarize the global effect of weak solute-water attractions on the HI.

While the translational correlation entropy apparently successfully explains the shape and main features of the HI potential, it offers no explanation for the maximum of the heat capacity at the DB [4,6,7]. The presence of this maximum is somewhat counterintuitive as it suggests that the state with lowest entropy and with the strongest stabilization of solvent positions with respect to the solute(s) is able to absorb the most thermal energy. However, the heat capacity increase may instead arise from soft modes appearing at the DB that do not involve translations with respect to the solute(s) position(s). In an analysis based on the average number of water neighbors and average pair potential energies, the maximum of the heat capacity has previously been described as arising from a counterplay between HB strengthening and enhanced HB breaking upon increasing temperature [6]. Here, we find that both the average number of neighbors in close contact and the average number of HB neighbors are independent of the interparticle separation, as shown in Fig. S5 in the Supplemental Material [16]. While there are enhanced fluctuations in both quantities at small separations, there is only small change at the DB ($d \sim 1$ Å).

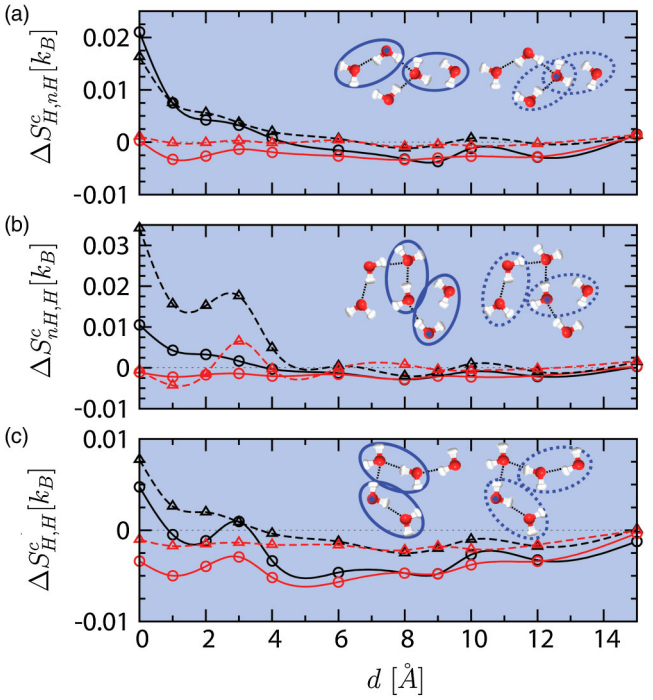

FIG. 4 (color online). (a) Triplet (dashed lines) and quadruplet (solid lines) correlation entropy difference of tagged HB and non-HB pairs: inner shell (black lines) and outer shell [dark gray (red) lines]. (b) Quadruplet correlation entropy difference of a tagged non-HB pair and its nearby HB pair, which is either HB (solid lines) or non-HB (dashed lines) to the tagged one. (c) Quadruplet correlation entropy difference of two nearby HB (solid lines) or non-HB (dashed lines) connected HB pairs. All quantities are expressed as a function of d relative to their values at $d = \infty$.

For the HS system in the region $d < 4$ Å, in which we observe HB strengthening and simultaneous softening of non-HB fluctuations, we may expect that many-body correlations will also be affected. Selected many-body correlation entropies are shown in Fig. 4. The correlations involving non-HB pairs [Figs. 4(a) and 4(b)] in the inner region are increased for $d < 4$ Å, which suggests that the relaxation of non-HB interactions arises from increased many-body correlations. In the case of HB quadruplets and nearby HB pairs [Fig. 4(c)], the many-body correlations are relaxed in both the inner and outer regions for $d > 4$ Å, while for $d < 4$ Å, they are increased in the inner and further relaxed in the outer region. Here, too, the global minimum is located at the DB. All many-body correlations in the hydration shell are strongly enhanced with respect to bulk water upon hydration of a single hydrophobic particle [14]. The present results indicate that the symmetry breaking in the hydration shell due to the presence of the second particle enables a net relaxation of many-body correlations in the outer region, while the remaining water molecules in the inner region become even more correlated. The most relaxed state is found at the DB, at which the outer shell is also most densely

packed. Appending the weak attractive solute-water interaction does not affect the above qualitative picture of the impact of enhanced many-body correlations. Quantitative differences will be addressed in detail in a separate publication.

Because of the extraordinary complexity of water, there may be more to the HI than can be captured by simplistic models such as the present, such as, for example, the nontrivial role of added dissolved gases [22]. However, the present results do suggest a new microscopic scenario for the changes in hydration water responsible for the HI. The main contribution to the HI is the relaxation of solute-water translational correlations, which is in agreement with suggestions in Ref. [23]. The contact is formed by the release of inner region molecules. Hydrogen bonds strengthen during the gradual association process. The DB is due to extremal solute-water translational correlations in the outer region, which arise as a response to the intrusion of water molecules from the inner region. At this distance, the fluctuations of non-HB interactions are largest and the many-body correlations are most relaxed. The free energy barrier to hydrophobic association is thus characterized by the densest packing of the outer region of the first hydration shell and softened collective fluctuations of HB clusters. This rearrangement renders the system entropically overall least relaxed, but excites soft collective fluctuations of nearby HB clusters, thus leading to the heat capacity maximum. The microscopic event governing the kinetics of hydrophobic association is therefore a relatively large critical collective fluctuation in the hydration water which pushes a substantial fraction of HB clusters from the inner to the outer region of the first hydration shell. The formation of contact relaxes the packing density and consequently the translational correlations with the solutes by releasing the surplus of water molecules into the bulk, thereby pushing the system into the global free energy minimum. The present results show that structural features and single molecule dynamics are not sufficient for understanding the microscopic origin of the HI. Rather, a complete description of hydrophobic association can be obtained only by explicitly considering collective fluctuations involving many-body correlations between water molecules.

*aljaz.godec@ki.si
†franci.merzel@ki.si

[1] C. Tanford, *The Hydrophobic Effect: Formation of Micelles and Biological Membranes* (Wiley, New York, 1973); W. Blokzijl and J. B. F. N. Engelberts, Angew. Chem., Int. Ed. Engl. **32**, 1545 (1993); B. Ben-Naim, *Hydrophobic Interactions* (Plenum, New York, 1980).
[2] F. H. Stillinger, Science **209**, 451 (1980); S. Garde and A. J. Patel, Proc. Natl. Acad. Sci. U.S.A. **108**, 16 491 (2011).
[3] D. Chandler, Nature (London) **437**, 640 (2005).
[4] D. E. Smith, L. Zhang, and A. D. J. Haymet, J. Am. Chem. Soc. **114**, 5875 (1992); D. A. Zichi and P. J. Rossky, J. Chem. Phys. **83**, 797 (1985); S. Shimizu and H. S. Chan, J. Chem. Phys. **113**, 4683 (2000); T. Ghosh, A. E. Garcia, and S. Garde, J. Chem. Phys. **116**, 2480 (2002); J.-L. Li, R. Car, C. Tang, and N. S. Wingreen, Proc. Natl. Acad. Sci. U.S.A. **104**, 2626 (2007); D. Paschek, J. Chem. Phys. **120**, 6674 (2004).
[5] G. Hummer, S. Garde, A. E. Garcia, A. Pohorille, and L. R. Pratt, Proc. Natl. Acad. Sci. U.S.A. **93**, 8951 (1996); L. R. Pratt, Annu. Rev. Phys. Chem. **53**, 409 (2002).
[6] D. Paschek, J. Chem. Phys. **120**, 10 605 (2004).
[7] S. W. Rick, J. Phys. Chem. B **107**, 9853 (2003); S. Shimizu and H. S. Chan, J. Am. Chem. Soc. **123**, 2083 (2001).
[8] P. T. Thomson, C. B. Davis, and R. H. Wood, J. Chem. Phys. **92**, 6386 (1988); R. H. Wood and P. T. Thomson, Proc. Natl. Acad. Sci. U.S.A. **87**, 946 (1990).
[9] N. Matubayasi, L. H. Reed, and R. M. Levy, J. Phys. Chem. **98**, 10 640 (1994); R. M. Lynden-Bell, N. Giovambattista, P. G. Debenedetti, T. Head-Gordon, and P. J. Rossky, Phys. Chem. Chem. Phys. **13**, 2748 (2011).
[10] H. S. Ashbaugh and L. R. Pratt, Rev. Mod. Phys. **78**, 159 (2006).
[11] K. Lum, D. Chandler, and J. D. Weeks, J. Phys. Chem. B **103**, 4570 (1999).
[12] D. Laage and J. T. Hynes, Science **311**, 832 (2006); D. Laage and J. T. Hynes, J. Phys. Chem. B **112**, 14 230 (2008).
[13] J. D. Eaves, J. J. Loparo, C. J. Fecko, S. T. Roberts, A. Tokmakoff, and P. L. Geissler, Proc. Natl. Acad. Sci. U.S.A. **102**, 13 019 (2005); M. Ji, M. Odelius, and K. J. Gaffney, Science **328**, 1003 (2010); D. Laage, G. Stirnemann, F. Sterpone, R. Rey, and J. Hynes, Annu. Rev. Phys. Chem. **62**, 395 (2011).
[14] A. Godec and F. Merzel, J. Am. Chem. Soc. **134**, 17 574 (2012).
[15] M. W. Mahoney and W. L. Jorgensen, J. Chem. Phys. **112**, 8910 (2000).
[16] See Supplemental Material at http://link.aps.org/supplemental/10.1103/PhysRevLett.111.127801 for details of applied concepts and additional results.
[17] A. Godec, J. C. Smith, and F. Merzel, Phys. Rev. Lett. **107**, 267801 (2011).
[18] D. T. Gillespie, Am. J. Phys. **51**, 520 (1983).
[19] D. E. Moilanen, D. Wong, D. E. Rosenfeld, F. E. Fenn, and M. D. Fayer, Proc. Natl. Acad. Sci. U.S.A. **106**, 375 (2009).
[20] T. Lazaridis, J. Phys. Chem. B **104**, 4964 (2000).
[21] T. Lazaridis and M. E. Paulaitis, J. Phys. Chem. **96**, 3847 (1992); T. Lazaridis, J. Phys. Chem. B **102**, 3531 (1998); **102**, 3542 (1998).
[22] B. W. Ninham and P. Lo Nostro, *Molecular Forces and Self Assembly: In Colloid, Nano Sciences and Biology* (Cambridge University Press, New York, 2010).
[23] T. Sumi and H. Sekino, J. Chem. Phys. **126**, 144508 (2007).